Journal of Power Sources 212 (2012) 220–225

Contents lists available at SciVerse ScienceDirect

Journal of Power Sources

journal homepage: www.elsevier.com/locate/jpowsour

The role of transition metals in non-precious nitrogen-modified carbon-based electrocatalysts for oxygen reduction reaction

Hyung-Suk Oh, Hansung Kim*

Dept. of Chemical and Biomolecular Engineering, Yonsei University, 50 Yonsei-ro, Seodaemun-gu, 120-749, Seoul, Republic of Korea

ARTICLE INFO

Article history:
Received 18 February 2012
Received in revised form
28 March 2012
Accepted 31 March 2012
Available online 16 April 2012

Keywords:
Non-precious metal catalyst
Oxygen reduction reaction
Transition metal
Active site
Polymer electrolyte membrane fuel cell

ABSTRACT

This study examines the role of transition metals (Co or Fe) on nitrogen-modified carbon-based catalysts for the oxygen reduction reaction (ORR). The nitrogen-modified carbon-based catalysts are synthesized by the pyrolysis process in the presence of polypyrrole (PPy) and ethylenediamine (ED) with different amounts of transition metals. Electrochemical data and inductively coupled plasma-atomic emission spectroscopy (ICP-AES) analysis do not support that the transition metal itself behaves as an active site for ORR. The X-ray photoelectron spectroscopy (XPS) and elemental analysis results show that the total nitrogen content and the active nitrogen functional groups, such as pyridinic-N and graphitic-N, are strongly dependent on the type of transition metal and the amount of transition metal used. Therefore, it is believed that transition metals serve to catalyze the formation of active nitrogen functional groups for the ORR by doping nitrogen into carbon.

1. Introduction

Recently, the development of inexpensive, non-precious, high-performance and durable oxygen reduction reaction (ORR) metal catalysts has become one of the major topics in research on polymer electrolyte membrane (PEM) fuel cells. One of the major drawbacks for the commercialization of PEM fuel cells is the high cost associated with the use of precious metal catalysts. Various materials have been studied for use as ORR catalysts, including transition metal chalcogenides [1–3], pyrolyzed transition metal macrocycles [4–7], conductive polymer-based catalysts [8–11], metal oxides/carbides [12–14] and transition metal nitrogen-containing complexes supported on carbon materials (M–N_x–C) [15–19]. Among these candidates, the M–N_x–C catalysts have gained increasing attention as a substitute to replace the currently used Pt-based electrocatalysts due to their promising ORR activity and stability in acidic environments and high potentials on cathode side.

The M–N_x–C catalyst has been extensively studied since it was demonstrated that transition metal macrocycles supported on carbon, such as cobalt phthalocyanine possess catalytic activity toward the ORR [20]. The stability of M–N_x–C catalyst in acidic condition was, however, not sufficient for its application in PEM fuel cells. In an effort to improve stability, high temperature heat treatment procedures were introduced to prepare the M–N_x–C catalysts [21–25]. The decomposed macrocyclic compounds still showed activity toward the ORR. A significant breakthrough came when it was discovered that M–N_x–C moieties could be created from a variety of different metal, nitrogen and carbon precursor materials with high heat treatment without using expensive macrocyclic compounds. Following this approach, many M–N_x–C catalysts have been synthesized using various inexpensive nitrogen-containing compounds such as ammonia, acetonitrile and chelating agents [26–29]. Recently, we reported highly active and stable M–N_x–C catalysts synthesized using chelating agents and conducting polymers as nitrogen precursors in the presence of transition metals [30].

Despite several decades of study by various groups, the nature of the active site and the role of the transition metal in M–N_x–C catalysts are still not clear and are heavily debated in the literature. Some researchers have proposed that transition metal atoms coordinated to nitrogen serve as active sites for the ORR [31,32]. In that scenario, the oxygen is initially adsorbed and reduced to peroxide at an M–N_x site. The intermediate product, peroxide, can be reduced to water by a decorated active metal oxide species on the catalyst surface [33]. Others have proposed that the transition metal itself does not play a role in the ORR. Instead, specific nitrogen functional groups such as pyridinic-N or graphitic-N serve as the catalytic site by enhancing the electron donor properties of the nitrogen-modified carbon-based catalysts [34–36]. Thus, ORR

* Corresponding author. Tel.: +82 2 2123 5753; fax: +82 2 312 6401.
E-mail address: elchem@yonsei.ac.kr (H. Kim).

0378-7753/$ – see front matter © 2012 Elsevier B.V. All rights reserved.
doi:10.1016/j.jpowsour.2012.03.098

catalytic activity depends on the nitrogen precursor, transition metal and synthesis strategy.

The present study explores the role of the transition metal in the synthesis of nitrogen-modified carbon-based ORR catalysts. The physical and electrochemical properties of the catalysts were characterized using various techniques. Based on these results, a hypothesis for the role of transition metals is proposed that can serve to guide the preparation of better nitrogen-modified carbon-based ORR catalysts for both activity and stability.

2. Experimental

2.1. Catalyst synthesis

The nitrogen-modified carbon-based ORR catalysts were synthesized by pyrolysis in the presence of cobalt, polypyrrole (PPy) and ethylenediamine (ED). This method was described in detail in our previous work [30]. As a first step, PPy coated carbon nanofiber composites (PPy–CNF) were synthesized by the in situ chemical oxidative polymerization of pyrrole monomers on CNF (from Suntel Co. Ltd., Korea). Separately, cobalt nitrate ($Co(NO_3)_2 \cdot 6H_2O$, as a Co source) was added to ethanol solutions in different amounts to prepare 2, 5, 10 and 20 wt.% Co loading on the PPy–CNF support. Next, ethylenediamine (ED) was added to the resulting ethanol solutions to prepare a cobalt–ethylenediamine (Co–ED) complex. The amount of ED added was the same for each solution to maintain the total amount of nitrogen source supplied constant during the synthesis procedure. Next, 0.2 g of PPy–CNF composite was added to each cobalt–ethylenediamine (Co–ED) solution, followed by vigorous stirring. The reaction mixtures were refluxed at 80 °C for 3 h, and the solvents were removed in a rotary evaporator at 50 °C under vacuum. The resulting powders were pyrolyzed in an argon atmosphere at 800 °C for 1 h. To remove excess metal remaining in the catalyst, the pyrolyzed samples were treated with a 0.5 M H_2SO_4 solution at 80 °C for 3 h before being washed thoroughly with de-ionized water. The resulting catalyst was designated as Co–ED/PPy–CNF-*M*, where *M* is the wt.% of the metal added during the reaction. For example, when 2, 5, 10 and 20 wt.% Co are added during the reaction, the samples are denoted as Co–ED/PPy–CNF-2, Co–ED/PPy–CNF-5, Co–ED/PPy–CNF-10 and Co–ED/PPy–CNF-20, respectively. For comparison, Fe instead of Co was used to prepare Fe–ED/PPy–CNF catalysts in the same fashion.

2.2. Electrochemical characterization and MEA test

Electrochemical characterization of the catalysts was performed using a rotating disk electrode (RDE, Pine Research Instrument). The experiment was performed in 0.5 M H_2SO_4 using a conventional three-electrode cell. A glassy carbon electrode with a thin film of the prepared sample was used as the working electrode. A platinum wire and standard $Hg/HgSO_4$ electrode were used as the counter and reference electrodes, respectively. The catalyst ink was prepared by blending the catalyst powder into a solvent of isopropyl alcohol (IPA) containing 5 wt.% Nafion ionomer. The catalyst ink was deposited onto the glassy carbon disk (0.35 mg cm^{-2}) followed by drying in a nitrogen atmosphere. Linear-sweep voltammograms were recorded in the potential range between 1.0 and 0.0 V_{NHE} at a scan rate 5 mV s^{-1} and 1200 rpm.

The membrane electrode assembly (MEA) preparation method is as follows. A commercial Pt/C catalyst (40 wt.% Pt, Johnson Matthey Co.) was used as the anode, and the various synthesized catalysts were used as the cathodes. The anode and cathode catalyst inks were prepared by ultrasonically mixing 5 wt.% Nafion ionomer in IPA, and then they were sprayed directly onto a Nafion 212 membrane with a 5 cm^2 geometric area. The total cathode loading was controlled at 8 mg cm^{-2}. The polarization curves were measured at 75 °C and 202.6 kPa absolute pressure. Pure hydrogen was supplied to the anode at a flow rate of 0.3 L min^{-1}, and pure oxygen was supplied to the cathode at a flow rate 0.6 L min^{-1}.

2.3. Physical characterization

High-resolution transmission electron microscopy (HR-TEM, JEM-30100 model) was performed to observe transition metal particles absorbed on the PPy–CNF supports. Inductively coupled plasma-atomic emission spectroscopy (ICP-AES) analysis was performed to estimate the transition metal loading in the catalysts. X-ray photoelectron spectroscopy (XPS, Sigma probe UK) was performed to analyze the surface composition of the catalysts. The binding energy (BE) scale was calibrated from the hydrocarbon contamination using the C 1s peak at 284.6 eV. The nitrogen content was measured using a Delta Plus mass spectrometer (Thermo Finnigan, Bremen, Germany) coupled with an elemental analyzer (EA 1110, CE Instruments, Milan, Italy).

3. Results and discussion

To investigate the role of cobalt in the nitrogen-modified carbon-based catalysts, Co–ED/PPy–CNF catalysts with varying amounts of Co were prepared. HR-TEM images in Fig. 1(a)–(d) shows Co–ED/PPy–CNF-2, Co–ED/PPy–CNF-5, Co–ED/PPy–CNF-10 and Co–ED/PPy–CNF-20 catalysts before the chemical leaching process, respectively. From these images, it appears that the number of cobalt particles increases with increasing cobalt loading from 2 to 20 wt.%. After the chemical leaching process, however, no significant difference was observed in terms of Co content from sample to sample as shown in Fig. 1(e)–(h). To quantify the Co content before and after the chemical leaching process in the catalysts, ICP analysis was carried out and the results are summarized in Table 1. Before chemical leaching, the Co content in each catalyst was close to the nominal target, ranging from 1.7 to 18 wt.%. In contrast, after chemical leaching the Co content that remained in the catalysts were reduced to between 1.0 and 3.2 wt.%. This result indicates that most of Co particles are dissolved and removed during the chemical leaching process. The chemical leaching process is essential for the application of fuel cells because the unstable Co in the acidic environment of fuel cells can cause contamination of the proton exchange membrane resulting in detrimental effects on the lifetime of fuel cells. As shown in the inset image of Fig. 1(e), the surviving Co particles are protected from the chemical leaching process by the encapsulation of several layers of graphitic carbon formed during the pyrolysis process [30].

The ORR catalytic activities for the Co–ED/PPy–CNF catalysts synthesized from varying amounts of Co were studied using a RDE system. First, all samples were treated by the chemical leaching process. For comparison, a catalyst with no added cobalt (Co–ED/PPy–CNF-0) was tested under the same conditions. As shown in Fig. 2, a significant improvement in activity is observed with increasing amounts of Co in the preparation of catalysts. The ORR current of the Co–ED/PPy–CNF-0 is 0.004 mA at 0.6 V_{NHE}. It is increased significantly to a value of 0.43 mA for the Co–ED/PPy–CNF-10. Beyond 10 wt.% Co loading, the current for the ORR is saturated. It is clear from the data that increasing the amount of the Co salt used in the preparation of catalysts increases the ORR activity. It is, however, still reasonable to assume that Co itself is not the direct ORR active site because ICP analysis and HR-TEM images show that the amount of Co remaining in the catalysts after the chemical leaching process is similar for all Co loading amounts. In

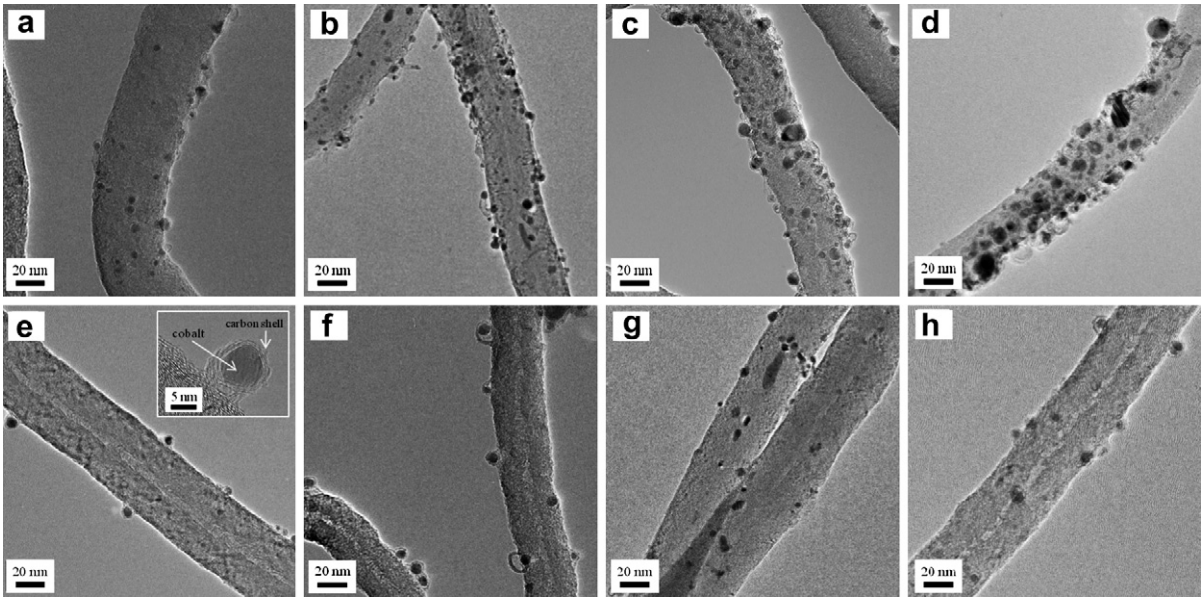

Fig. 1. HR-TEM images of the nitrogen-modified carbon-based catalysts with different Co contents. (a) Co–ED/PPy–CNF-2, (b) Co–ED/PPy–CNF-5, (c) Co–ED/PPy–CNF-10 and (d) Co–ED/PPy–CNF-20 before chemical leaching. (e) Co–ED/PPy–CNF-2, (f) Co–ED/PPy–CNF-5, (g) Co–ED/PPy–CNF-10 and (h) Co–ED/PPy–CNF-20 after chemical leaching.

addition, the surviving Co particles are covered with graphene layers [37–39].

To understand the role of Co in more detail, the total nitrogen content and the N 1s level of each catalyst were measured by elemental and XPS analysis, respectively. According to these results, as shown in Fig. 3, both the total nitrogen content and the type of nitrogen functional groups in the catalysts are strongly affected by the initial amount of Co before the chemical leaching process. The total nitrogen content increases from 1 to 4.5 wt.% with increased initial Co loading up to 10 wt.%. The catalyst with 20 wt.% Co loading does not show a significant difference from that of the catalyst loading with 10 wt.%. This result follows the same trend as the ORR activity in Fig. 2, indicating that a higher nitrogen content in the catalyst leads to a higher ORR activity [40]. Co also has an influence on the type of nitrogen functional groups present. The N 1s spectra obtained from the XPS are deconvoluted into three peaks. Those three peaks are pyridinic-N (398.5 eV), pyrrolic-N (400.5 eV) and graphitic-N (401.1 eV) [41,42]. From the XPS results it is clear that the ratios of both pyridinic-N and graphitic-N increase, whereas that of pyrrolic-N decreases as more Co is introduced during the reaction. It has been proposed that both pyridinic-N and quaternary-N are responsible for the ORR active sites [43]. It is worth noting that the total amount of nitrogen applied to synthesize each catalyst is held constant by fixing the amount of PPy and ED used. Therefore, it could be concluded that Co behaves as a booster to increase nitrogen content in the catalyst by creating more nitrogen functional groups that are active toward the ORR from the nitrogen sources added initially.

To investigate the effect of another transition metal, Fe–ED/PPy–CNF catalysts with different Fe contents were synthesized by the same process used in the preparation of Co–ED/PPy–CNF. Fe is selected because it is also known to be an efficient metal in the preparation of nitrogen-modified carbon-based catalysts. The ORR catalytic activities for these catalysts are measured using the RDE test and the results are presented in Fig. 4 and Table 2. All of the samples are chemically leached before testing. After chemical leaching, the content of Fe is reduced to below 2 wt.%, implying that most of Fe was dissolved as is the case for Co in the Co–ED/PPy–CNF catalysts. The ORR activity of Fe–ED/PPy–CNF increases as the amount of Fe increases. This result is the same trend of

Table 1
Cobalt (Co) content and catalytic activity in the nitrogen-modified carbon-based ORR catalysts. ICP was used to determine Co content and was obtained before and after chemical leaching in a 0.5 M H_2SO_4 solution at 80 °C. Catalytic activity was determined using a RDE system.

Sample	Co content (wt.%)		Onset potential (V_{NHE})	Current @ 0.6 V_{NHE} (mA)
	Before leaching	After leaching		
Co–ED/PPy–CNF-0	0	0	0.64	0.004
Co–ED/PPy–CNF-2	1.7	1.0	0.79	0.061
Co–ED/PPy–CNF-5	4.1	2.1	0.80	0.187
Co–ED/PPy–CNF-10	8.2	2.7	0.87	0.430
Co–ED/PPy–CNF-20	18.0	3.2	0.85	0.375

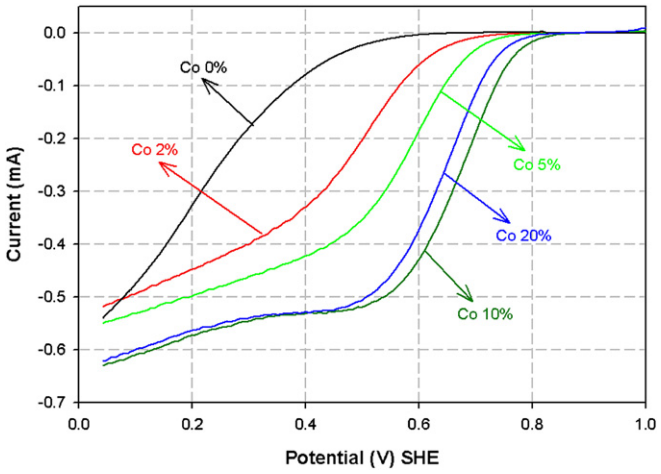

Fig. 2. Polarization curves of oxygen reduction on the nitrogen-modified carbon-based catalysts with different Co contents. For comparison, the curve measured on the catalyst with no cobalt loading (Co–ED/PPy–CNF-0) is also shown. The measurements were performed in an O_2-saturated 0.5 M H_2SO_4 solution using a potential scan rate of 5 mV s^{-1} and a rotation speed of 1200 rpm.

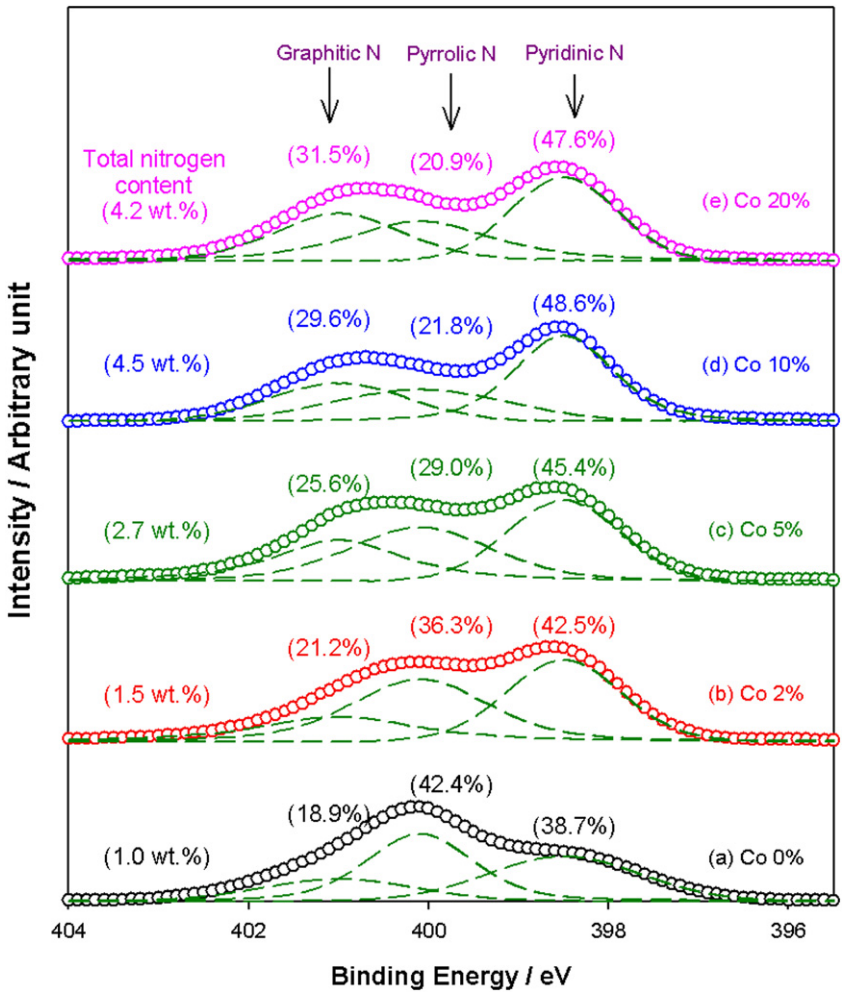

Fig. 3. The total nitrogen content as determined by elemental analysis, and deconvoluted XPS spectra of the N 1s region for (a) Co–ED/PPy–CNF-0, (b) Co–ED/PPy–CNF-2, (c) Co–ED/PPy–CNF-5, (d) Co–ED/PPy–CNF-10 and (e) Co–ED/PPy–CNF-20.

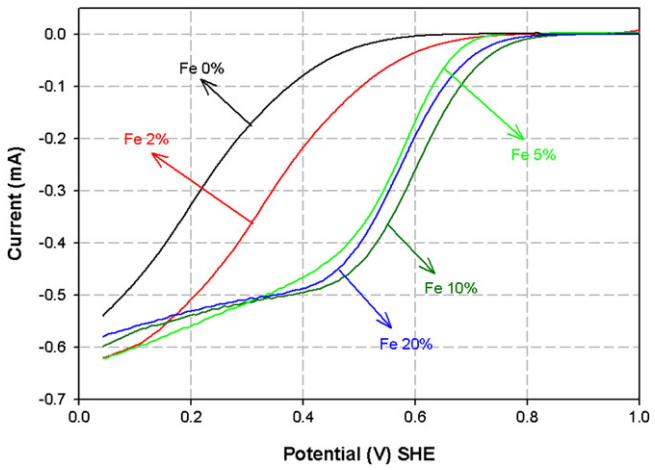

Fig. 4. Polarization curves for oxygen reduction on the nitrogen-modified carbon-based catalysts with different Fe contents. For comparison, the curve measured on the catalyst with no iron loading (Fe–ED/PPy–CNF-0) is also shown. The measurements were performed in an O_2-saturated 0.5 M H_2SO_4 solution using a potential scan rate of 5 mV s^{-1} and a rotation speed of 1200 rpm.

Co–ED/PPy–CNF catalysts in Fig. 2, but the performance of the ORR is lower for Fe–ED/PPy–CNF than for Co–ED/PPy–CNF. To investigate the nitrogen functional groups in Fe–ED/PPy–CNF, XPS and elemental analysis are once again carried out and the results are shown in Fig. 5. The total nitrogen content of the catalysts increases with Fe content and the Fe–ED/PPy–CNF-10 catalyst shows the highest N content of 3.2 wt.%. This result displays the same trend as with the Co–ED/PPy–CNF as shown in Fig. 3, but Fe–ED/PPy–CNF had an overall lower nitrogen content when compared with Co–ED/PPy–CNF. The XPS results show that the ratios of pyridinic-N and graphitic-N increase while that of pyrrolic-N decreases as Fe is introduced. In particular, the ratio of graphitic-N for the Fe–ED/

Table 2
Iron (Fe) content and catalytic activity in the nitrogen-modified carbon-based ORR catalysts. ICP was used to determine Fe content and was obtained before and after chemical leaching in a 0.5 M H_2SO_4 solution at 80 °C. Catalytic activity was determined using a RDE system.

Sample	Fe content (wt.%)		Onset potential (V_{NHE})	Current @ 0.6 V_{NHE} (mA)
	Before leaching	After leaching		
Fe–ED/PPy–CNF-0	0	0	0.64	0.004
Fe–ED/PPy–CNF-2	1.3	0.7	0.78	0.040
Fe–ED/PPy–CNF-5	3.8	1.5	0.80	0.168
Fe–ED/PPy–CNF-10	8.0	1.8	0.86	0.261
Fe–ED/PPy–CNF-20	15.3	2.0	0.83	0.195

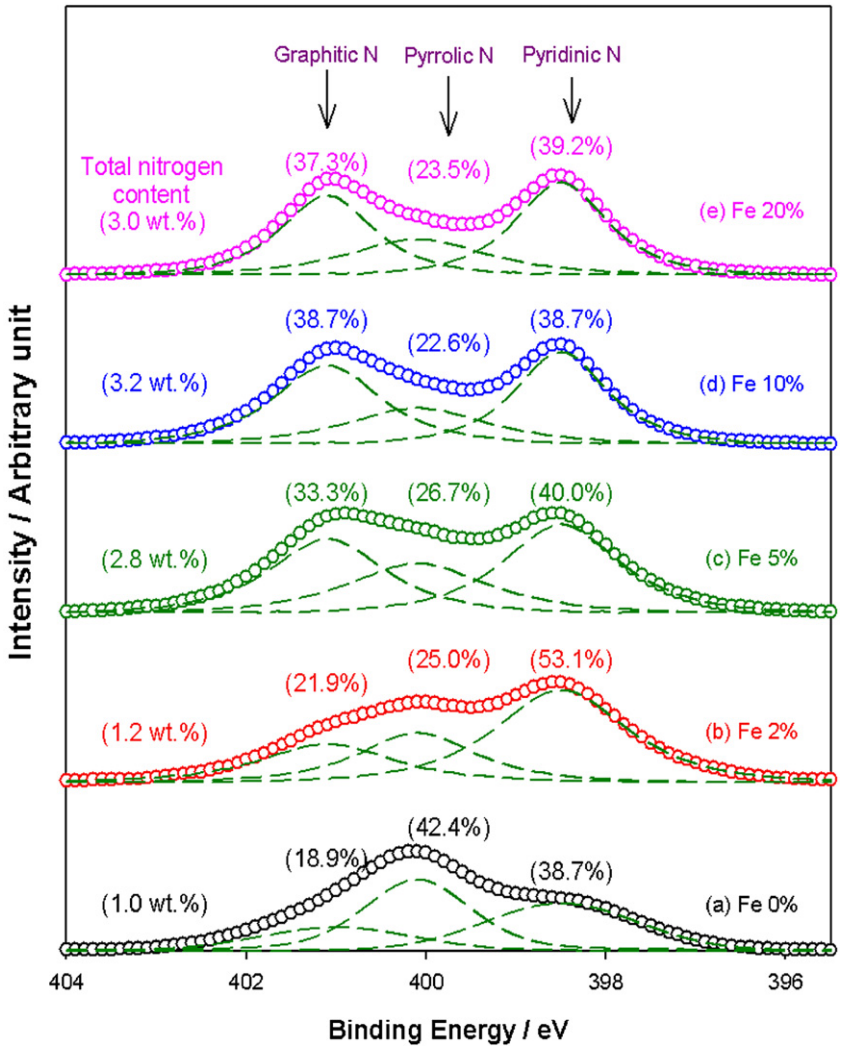

Fig. 5. The total nitrogen content as determined by elemental analysis, and deconvoluted XPS spectra of the N 1s region for (a) Fe–ED/PPy–CNF-0, (b) Fe–ED/PPy–CNF-2, (c) Fe–ED/PPy–CNF-5, (d) Fe–ED/PPy–CNF-10 and (e) Fe–ED/PPy–CNF-20.

PPy–CNF catalysts increases more than in the case of the Co–ED/PPy–CNF catalysts. In a summary of experimental results obtained from Co–ED/PPy–CNF and Fe–ED/PPy–CNF, it can be concluded that transition metals such as Co and Fe do not act as an active site for the ORR. Instead, they serve to promote the formation of active nitrogen functional groups for the ORR by incorporating nitrogen into the carbon structure during pyrolysis. After pyrolysis, the metals should be removed to avoid contaminating the fuel cells. Because the metals are not an active site of ORR, catalysts still showed high ORR activity after the chemical leaching process.

To correlate the results of XPS and the ORR activity further, the MEAs using Co–ED/PPy–CNF-10 and Fe–ED/PPy–CNF-10 catalysts were fabricated and their polarization curves were measured using a fuel cell station. All catalysts were chemically leached nitrogen-modified carbon-based catalysts. As shown in Fig. 6, the open circuit voltages of these cells are approximately 0.85 V. The Co-based catalyst is more active toward the ORR than the Fe-based catalyst, a result in good agreement with RDE test results. The Co–ED/PPy–CNF-10 shows as much as 0.7 A cm^{-2} at 0.4 V, compared to only 0.53 A cm^{-2} for the Fe–ED/PPy–CNF-10 at the same potential. This is due to the difference in the quantity of the active nitrogen content derived from the use of different transition metals.

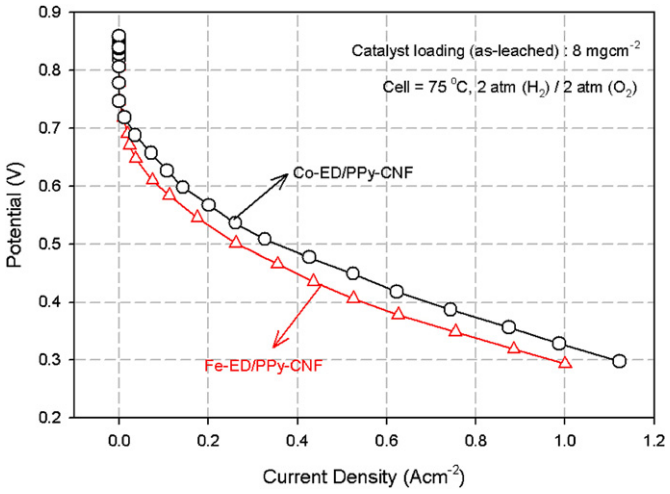

Fig. 6. Comparison of MEA performance using the Co–ED/PPy–CNF-10 and Fe–ED/PPy–CNF-10. The cathode catalyst loading was 8.0 mg cm^{-2}. The experiments were performed under 2 atm using H_2/O_2 for the anode and cathode.

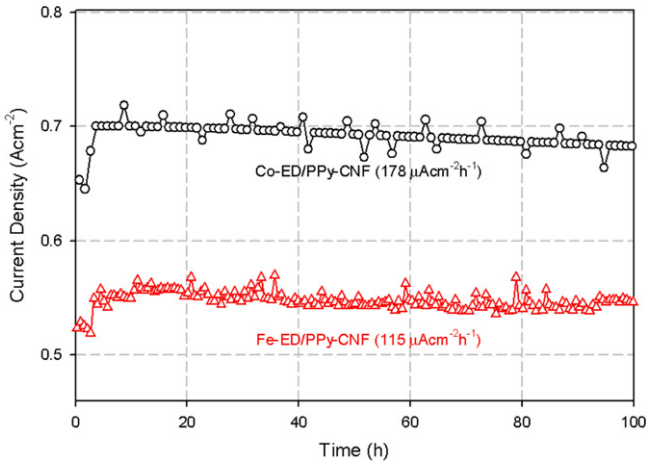

Fig. 7. Stability test of H_2/O_2 fuel cells at 0.4 V using Co–ED/PPy–CNF-10 and Fe–ED/PPy–CNF-10 catalysts as the cathode catalysts for 100 h.

Fig. 7 displays the stability tests of the MEAs with Co–ED/PPy–CNF-10 and Fe–ED/PPy–CNF-10 catalysts performed at 0.4 V for 100 h. The MEA performance of each catalyst decreases continuously with different degradation rates as a function of time. The Co–ED/PPy–CNF-10 catalyst shows a performance degradation rate of 178 μA cm^{-2} h^{-1}, while the Fe–ED/PPy–CNF-10 degrades at approximately 115 μA cm^{-2} h^{-1}. This difference of degradation rate can be explained by the difference in nitrogen functional groups for the catalysts. It is well known that both pyridinic-N and graphitic-N are active for the ORR [44]. In terms of stability, the graphitic-N is preferred to the pyridinic-N. The pyridinic-N is not stable in an acidic environment because it can be protonated to yield a pyridinic-N–H that is not active toward the ORR. In contrast, the graphitic-N has bonds to three carbon atoms, resulting in a decreased likelihood of protonation [45]. Because the Fe–ED/PPy–CNF-10 has a higher ratio of graphitic-N when compared with Co–ED/PPy–CNF-10, it is expected that Fe–ED/PPy–CNF-10 would be more stable than Co–ED/PPy–CNF-10.

4. Conclusion

In this study, the role of the transition metal (Co or Fe) in nitrogen-modified carbon-based catalysts for the ORR is explored. The nitrogen-modified carbon-based catalysts are synthesized by the pyrolysis process in the presence of PPy and ED with varying transition metal contents. Based on electrochemical and quantitative analysis, it is believed that the transition metal itself does not participate directly as the active site for the ORR. Instead, the transition metal promotes the formation of active sites by catalyzing the incorporation of nitrogen atoms into the graphene layers to replace carbon atoms during pyrolysis. In a comparison between Co and Fe, it is found that Co is more effective in increasing the nitrogen content and active nitrogen functional groups than Fe, resulting in higher ORR activity. Fe derived catalysts, however, show higher durability due to the enhanced formation of graphitic nitrogen that is more stable in the acidic media than pyridinic nitrogen. Therefore, it is important to find effective transition metal to improve activity and durability of nitrogen-modified carbon-based catalysts.

Acknowledgments

This work was supported by Human Resources Development and New & Renewable Energy of the Korea Institute of Energy Technology Evaluation and Planning (KETEP) grant funded by the Korea government Ministry of Knowledge Economy (No. 20104010100500, No. 20093021030021) and the Priority Research Centers Program through the National Research Foundation of Korea (2009-0093823)

References

[1] E. Vayner, R.A. Sidik, A.B. Anderson, B.N. Popov, J. Phys. Chem. C 111 (2007) 10508–10513.
[2] Y.J. Feng, T. He, N. Alonso-Vante, Chem. Mater. 20 (2008) 26–28.
[3] R.A. Sidik, A.B. Anderson, J. Phys. Chem. B 110 (2006) 936–941.
[4] A.L. Bouwkamp-Wijnoltz, W. Visscher, J.A.R. van Veen, Electrochim. Acta 43 (1998) 3141–3152.
[5] M. Ladouceur, G. Lalande, D. Guay, J.P. Dodelet, L. Dignardbailey, M.L. Trudeau, R. Schulz, J. Electrochem. Soc. 140 (1993) 1974–1981.
[6] P. Gouerec, M. Savy, Electrochim. Acta 44 (1999) 2653–2661.
[7] S.L. Gojkovic, S. Gupta, R.F. Savinell, Electrochim. Acta 45 (1999) 889–897.
[8] R. Bashyam, P. Zelenay, Nature 443 (2006) 63–66.
[9] K. Lee, L. Zhang, H. Lui, R. Hui, Z. Shi, J.J. Zhang, Electrochim. Acta 54 (2009) 4704–4711.
[10] W.M. Millan, T.T. Thompson, L.G. Arriaga, M.A. Smit, Int. J. Hydrogen Energy 34 (2009) 694–702.
[11] H.S. Liu, Z. Shi, J.L. Zhang, L. Zhang, J.J. Zhang, J. Mater. Chem. 19 (2009) 468–470.
[12] H. Meng, P.K. Shen, Electrochem. Commun 8 (2006) 588–594.
[13] X.G. Yang, C.Y. Wang, Appl. Phys. Lett. 86 (2005) 224104-1–224104-3.
[14] K.D. Nam, A. Ishihara, K. Matsuzawa, S. Mitsushima, K. Ota, Electrochem. Solid-State Lett. 12 (2009) B158–B160.
[15] M. Lefevre, E. Proietti, F. Jaouen, J.P. Dodelet, Science 324 (2009) 71–74.
[16] C.W.B. Bezerra, L. Zhang, K.C. Lee, H.S. Liu, J.L. Zhang, Z. Shi, A.L.B. Marques, E.P. Marques, S.H. Wu, J.J. Zhang, Electrochim. Acta 53 (2008) 7703–7710.
[17] K. Gong, F. Du, Z. Xia, M. Durstock, L. Dai, Science 323 (2009) 760–764.
[18] U.I. Kramm, I. Herrmann-Geppert, P. Bogdanoff, S. Fiechter, J. Phys. Chem. C 115 (2011) 23417–23427.
[19] R. Liu, D. Wu, X. Feng, K. Müllen, Angew. Chem., Int. Ed. 49 (2010) 2565–2569.
[20] R. Jasinski, Nature 201 (1964) 1212–1213.
[21] E. Yeager, Electrochim. Acta 29 (1984) 1527–1537.
[22] K. Wiesener, Electrochim. Acta 31 (1986) 1073–1078.
[23] S. Ye, A.K. Vijh, Int. J. Hydrogen Energy 30 (2005) 1011–1015.
[24] H.J. Zhang, X. Yuan, L. Sun, X. Zeng, Q.Z. Jiang, Z. Shao, Z.F. Ma, Int. J. Hydrogen Energy 35 (2010) 2900–2903.
[25] Y. Ji, Z. Li, S. Wang, G. Xu, X. Yu, Int. J. Hydrogen Energy 35 (2010) 8117–8121.
[26] P.H. Matter, U.S. Ozkan, Catal. Lett. 109 (2006) 115–123.
[27] P.H. Matter, L. Zhang, U.S. Ozkan, J. Catal. 239 (2006) 83–96.
[28] P.H. Matter, E. Wang, J.M.M. Millet, U.S. Ozkan, J. Phys. Chem. C 111 (2007) 1444–1450.
[29] R.A. Sidik, A.B. Anderson, N.P. Subramanian, S.P. Kumaraguru, B.N. Popov, J. Phys. Chem. C 110 (2006) 1787–1793.
[30] H.S. Oh, J.G. Oh, B. Roh, I. Hwang, H. Kim, Electrochem. Commun 13 (2011) 879–881.
[31] M. Lefèvre, J.P. Dodelet, P. Bertrand, J. Phys. Chem. B 104 (2000) 11238–11247.
[32] K. Sawai, N. Suzuki, J. Electrochem. Soc. 151 (2004) A682–A688.
[33] T.S. Olson, S. Pylypenko, J.E. Fulghum, P. Atanassov, J. Electrochem. Soc. 157 (2010) B54–B63.
[34] N.P. Subramanian, X. Li, V. Nallathambi, S.P. Kumaraguru, H. Colon-Mercado, G. Wu, J.-W. Lee, B.N. Popov, J. Power Sources 188 (2009) 38–44.
[35] R. Kothandaraman, V. Nallathambi, K. Artyushkova, S.C. Barton, Appl. Catal. B: Environ. 92 (2009) 209–216.
[36] S. Kundu, T.C. Nagaiah, W. Xia, Y. Wang, S.V. Dommele, J.H. Bitter, M. Santa, G. Grundmeier, M. Bron, W. Schuhmann, M. Muhler, J. Phys. Chem. C 113 (2009) 14302–14310.
[37] G. Wu, C. Dai, D. Wang, D. Li, N. Li, J. Mater. Chem. 20 (2010) 3059–3068.
[38] G. Liu, X.G. Li, P. Ganesan, B.N. Popov, Appl. Catal. B: Environ. 93 (2009) 156–165.
[39] V. Nallathambi, J.W. Lee, S.P. Kumaraguru, G. Wu, B.N. Popov, J. Power Sources 183 (2008) 34–42.
[40] H.-S. Oh, J.-G. Oh, W.H. Lee, H.-J. Kim, H. Kim, Int. J. Hydrogen Energy 36 (2011) 8181–8186.
[41] K. Stańczyk, R. Dziembaj, Z. Piwowarska, S. Witkowski, Carbon 33 (1995) 1383–1392.
[42] R.J.J. Jansen, H. van Bekkum, Carbon 33 (1995) 1021–1027.
[43] H. Kim, K. Lee, S.I. Woo, Y. Jung, Phys. Chem. Chem. Phys. 13 (2011) 17505–17510.
[44] S. Yang, X. Feng, X. Wang, K. Müllen, Angew. Chem., Int. Ed. 50 (2011) 5339–5343.
[45] G. Liu, X. Li, P. Ganesan, B.N. Popov, Electrochim. Acta 55 (2010) 2853–2858.